AMS Bologna
Internal Note
2001–03–01

AMS Time of Flight System Performances During the STS-91 Shuttle Flight

Diego Casadei[1]
Dipartimento di Fisica, Università di Bologna, via Irnerio 46, I-40126 Bologna, Italy

April 24, 2001

ABSTRACT

This paper shows the performances of the time of flight system (TOF) of the AMS detector during the NASA STS-91 flight. The TOF system has to give the fast trigger signal to the detector and to measure the particle velocity and charge. Its time resolution (1 standard deviation) is 120 ps for protons and better for ions with $Z > 1$, and it is able to distinguish between singly and doubly charged particles within 1%. In addition, the TOF measurements alone can be used to buid a simplified data analysis.

Subject headings: AMS: trigger, time of flight.

Contents

1. Introduction

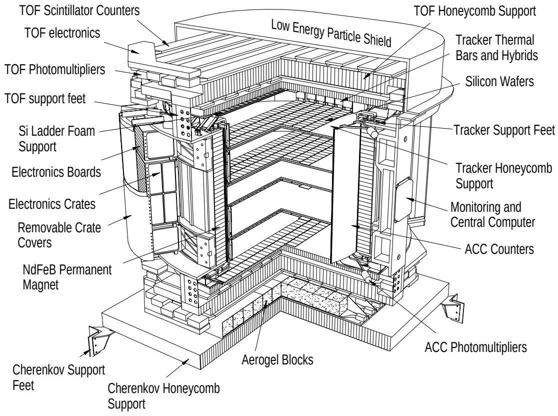

Figure 1. The AMS-1 detector for the STS-91 mission.

The *Alpha Magnetic Spectrometer* (AMS) [1] is a particle detector that will be installed on the International Space Station in 2003, and will measure cosmic ray fluxes for at least three years.

During the precursor flight (NASA STS-91 mission, 2–12 June 1998), aboard of the shuttle Discovery, AMS collected data for about 180 hours. Figure 1 shows the first version of the detector, consisting of a permanent Nd-Fe-B magnet enclosing four of the six silicon tracker planes and the anticoincidence scintillator counters, four layers of scintillator counters that constitute the time of flight (TOF) system, and a threshold aerogel Čerenkov detector.

---

[1] `Diego.Casadei@bo.infn.it`

The TOF system was completely designed and built at the INFN Laboratories in Bologna. Its main issues are: 1) giving the fast trigger to AMS readout electronics, and measuring 2) the particle to light speed ratio β, 3) the particle direction, 4) crossing position and 5) charge. In addition, it had to operate in space with severe limits for weight and power consuption.

Each TOF plane has 14 scintillator counters covering a roughly circular area of 1.6 m^2, and every counter has 3 Hamamatsu R5900 photomultipliers per side, whose signals are summed to have a good redundancy and light collection efficiency. The total power consumption of the system (112 channels, 336 phototubes) was 150 W, while its weight (support structure included) was 250 kg [2, 3].

In the following sections, the TOF system behavior will be examined from two points of view: the trigger efficiency and the quality of the TOF measurements.

2. The AMS trigger

AMS has two levels of trigger logic. The "first level" processes only the scintillators data in a very fast way, then the tracker information is used. The tracker response is about two order of magnitude slower than the scintillators one, hence there is enough time to do a more complex on-fly analysis. The second level is then called "third level trigger". Figure 2 shows the impact of the different trigger conditions on data taken requiring only the fast trigger ("prescaled events").

In order the event to be acquired, the first condition (called "fast trigger") is the coincidence of the four TOF planes. If within the next 200 ns one among the other conditions is not satisfied, the event is discarded and AMS waits for another fast trigger. Figure 2 shows that about a 0.5% of the fast triggers is due to noise (compare the second to the first bin in the histogram).

The fast trigger requires at least a signal from one side of one TOF counter in each plane. The coincidence of both sides of the counters used by the fast trigger and the existence of only one or two adjacent hitted counters in the first three planes, will be checked by the third level trigger. This consistency test alone would discard about a 30% of the fast triggers.

The next first level trigger condition, called "matrix condition", simply discards all the tracks that have no way to intersect the tracker[2], that had a geometrical acceptance of about 0.16 m^2 sr. Only 85% of the fast triggers survives to this cut.

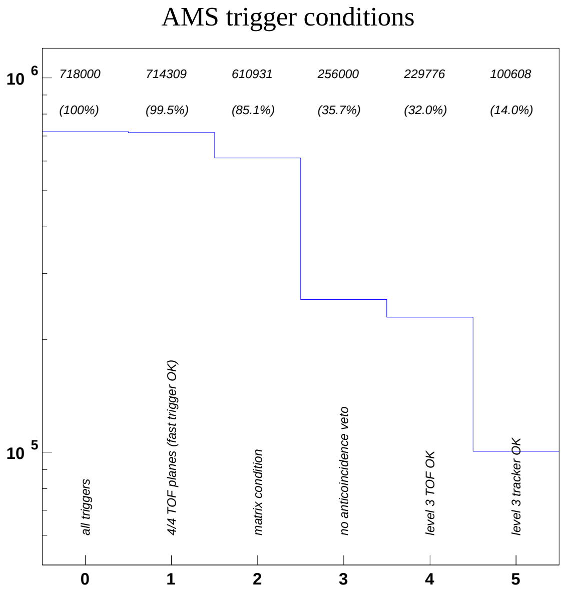

Figure 2. Trigger cuts on prescaled events.

The last condition at the first level trigger is the absence of signal from the anticoincidence counters (36% of the fast triggers).

The third level trigger, in addition to the consistency of the TOF counters data, applies a cut on the maximum curvature of the trajectory (sixth bin of figure 2), leaving 14% of the triggers. This is the number of collected events.

3. Fast trigger

The *fast trigger* (FT) signal is generated when at least one counter side of each TOF plane gives a signal. It is the very first step of the trigger logic, used both to start its clock and to participate in the first level trigger with the signals from the anticoincidence scintillators. AMS is locked between the FT and "clear" signals, that comes after 200 ns if the first level condition is not satisfied, or later if the event satisfies this condition. The maximum delay between these two signal is roughly 400 μs, corresponding to the acquisition of a "good event" (i.e. an event that survives to all trigger conditions). This delay is the "dead time" of the AMS detector.

To measure the efficiency and background of the FT signal one needs a way to independently measure inci-

---

[2] The tracker was not complete at the time of STS-91 mission: only a subset was mounted on AMS for the test flight.

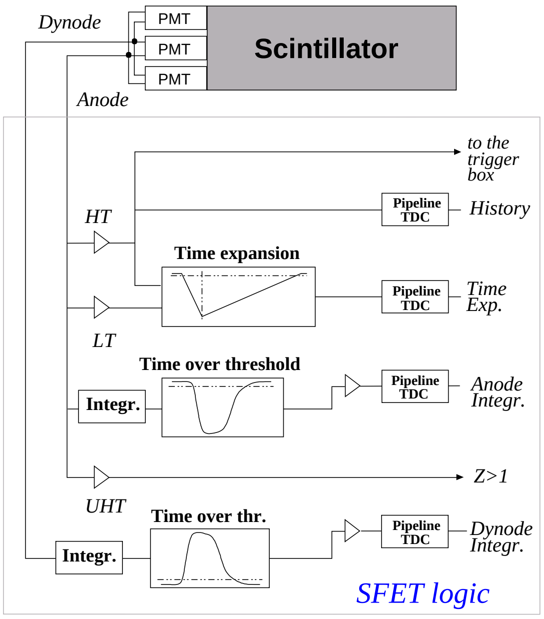

Figure 3. Logic of the SFET board [4].

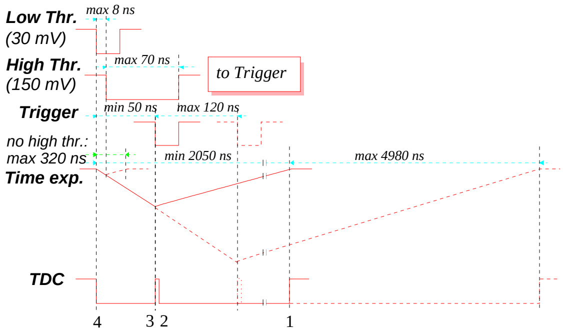

Figure 4. The TDC of the SFET board [4].

dent particles. AMS is able to do this by exploiting a feature of the TOF electronic boards [4] (called SFET boards): the existence of never locked channels.

3.1. Off-time events

From each TOF counter side the anode and the last dynode pulses are read. They go to a SFET board, where the dynode signal is integrated while the anode signal is split into three channels, called "anode integrator", "time expansion" and "history" (see figure 3).

The anode integration is done by charging a capacitor and measuring its discharge time, with a threshold corresponding to 0.3 MeV of energy deposition in the counter (the dynode integration is similar). This time is a logarithmic function of the charge deposited in the capacitor.

The anode signal is also sent to a comparator with a threshold[3] set to 30 mV ("low threshold", LT) that starts a TDC and the charging of another capacitor. If within the next 8 ns this pulse doesn't pass a threshold at 150 mV ("high threshold", HT) the signal is considered as "noise" and nothing happens. In the other case, the board will wait (at least 50 ns and at most 120 ns) for a FT signal coming from the trigger logic: the FT stops the capacitor charging and starts its discharging (figure 4).

The TDC measures the charging and discharging times, the latter being roughly 40 times longer than the former, and then it is locked until it receives a signal called "common stop", generated 6.5 μs after the FT by the SFET logic. This is the "time expansion" channel.

The "history" channel corresponds to the time over the high threshold, and it is always active, like the anode and dynode integrator channels. The corresponding TDCs have 14 bits words, a clock of 1 GHz and a buffer of 16 fronts, so that the total available time-window is about 16.5 μs. In this way these channels are able to record 8 signals (1 up and 1 down front) starting from 10 μs before the FT, ending 6.5 μs after it. Only one history signal is time-correlated to the time expansion one, while all the others are called *off-time signals*.

Then we can search for off-time signals in both sides of a counter, and in correlation with a single counter in all the other TOF planes, requiring both the anode and the history (i.e. HT) signals [5]. In this way we obtain the tracks of particles that traversed the TOF system during the dead time, i.e. the *off-time events*.

3.2. Fast trigger efficiency and background

By means of the off-time events, one can estimate the fast trigger efficiency. In the average, there are $0.05 \div 0.7$ off-time events per trigger, depending on the trigger rate. Figure 5 shows that the fast trigger efficiency , for the whole duration of the STS-91 flight, is always greater than 99.8%.

As noticed in the previous section, the background can be estimated looking at the prescaled events, taken

---

[3] A MIP signal has a peak at about 300 mV.

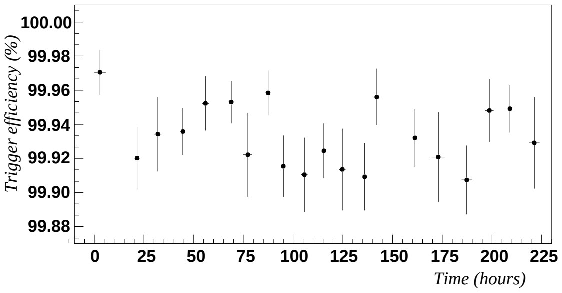

Figure 5. Fast trigger efficiency during the STS-91 shuttle flight.

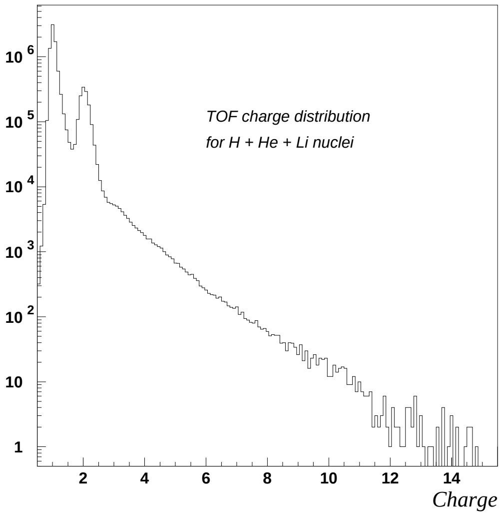

Figure 6. TOF charge distribution for $Z < 4$ nuclei.

by AMS in the ratio 1 to 1000 normal triggers. Figure 2 shows that about 0.5% of the fast triggers were due to noise, but this background is eliminated by requiring the coincidence of both sides of the same counter in the third level trigger.

4. Particle separation

At the trigger level, one goal of the TOF system was to give a special flag for ions. Then it was designed to be able to distinguish in a fast and efficient way protons and “$Z > 1$” particles.

Even though the low power electronics of the SFET boards was not optimized for a good charge measurement, the TOF system energy loss measurement is sufficient to separate singly by doubly charged particles with a contamination at the level of 1%, as figure 6 shows.

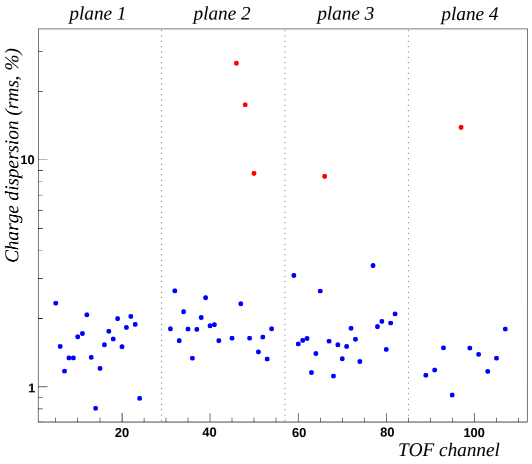

Figure 7. TOF charge peaks dispersion during the STS-91 flight.

The stability of the charge measurement is very good for all the 112 TOF channels, but four channels (see figure 7).

One of the most important things the TOF system has to do is to separate downward from upward going particles: a Helium nucleus wrongly said “upward” would be interpreted as an anti-Helium nucleus.

The average time of flight of particles traversing AMS is of the order of 5 ns, while the time measurement has a standard deviation of roughly 0.1 ns. Thus the probability to do a mistake (i.e. to have a time measurement 10 ns wrong) is extremely low, as shown in figure 8.

5. Charge resolution

The TOF scintillator counters are read by 3 photomultipliers at each end, allowing a precise time of flight measurement and a basic energy deposition measurement, whose aim was to discriminate in a very fast way between protons and all other cosmic rays ions, in order to be able to use this information at the first level trigger.

Due to the strong constraints about power consuption, the TOF front-end electronics was not optimized for an energy deposition measurement, resulting in a

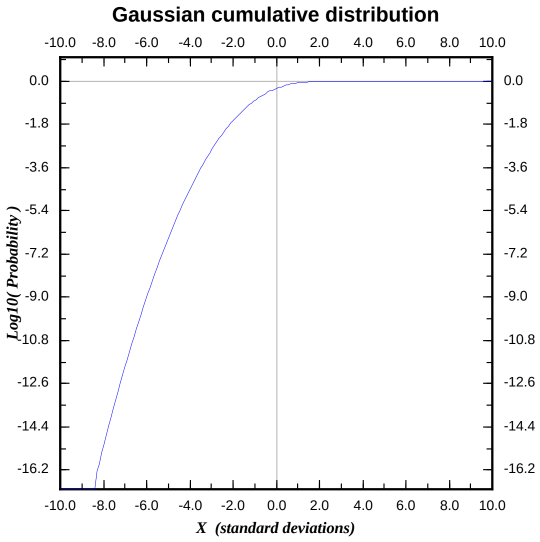

Figure 8. The probability of misunderstanding down-going particles, as function of the number of standard deviations from the mean time of flight is given by the “error function”.

good separating power between charges $|Z| = e$ and $|Z| > e$ (where e is the proton charge) but a poor charge resolution for $|Z| > 2e$ (see figure 6).

In order to convert the TOF energy deposition measurement into a charge measurement, one first divides the energy loss distribution by a Bethe-Bloch function without the particle charge Z^2 term, and then tooks the square root, obtaining the measured charge distribution. The adopted form for the Bethe-Bloch function is [6]:

$$-\frac{\mathrm{d}E}{\mathrm{d}x} = K\left\langle\frac{Z}{A}\right\rangle_{\mathrm{scint}}\frac{Z^2}{\beta^2}\left[\frac{1}{2}\ln\frac{2m_ec^2(\beta\gamma)^2T_{\max}}{\langle I\rangle^2}-\beta^2-\frac{\delta}{2}\right] \qquad (1)$$

with $K = 0.307075\,\mathrm{MeV\,g^{-1}\,cm^2}$, and

$$T_{\max} = \frac{2m_ec^2\beta^2\gamma^2}{1+2\gamma m_e/M+(m_e/M)^2}\,. \qquad (2)$$

The density effect correction is computed using the Sternheimer parametrization [7]:

$$\delta = \begin{cases} 2(\ln 10)x-\overline{C}, & x \geq x_1 \\ 2(\ln 10)x-\overline{C}+a(x_1-x)^k, & x_0 \leq x < x_1 \\ 0, & x < x_0 \end{cases} \qquad (3)$$

where $x \equiv \log_{10}\beta\gamma$ and $\overline{C}$ is equal to the constant $-C$ tabulated by Sternheimer et al. [8].

param.	value
Z/A	0.54141
ρ	$1.032\,(\mathrm{g/cm^3})$
$\langle I\rangle$	$84\,(\mathrm{eV})$
x_0	0.1464
x_1	2.4855
$\overline{C}$	3.1997
a	0.16101
k	3.2393
B_1	0.01
B_2	5×10^{-5}

Table 1. Parameters values for the TOF Bicron BC408 (polyvinyltoluene) counters from [8].

The Birk’s saturation effect is also included, obtaining for the light emitted per unit length:

$$-\frac{\mathrm{d}L}{\mathrm{d}x} = \frac{A\left(-\frac{\mathrm{d}E}{\mathrm{d}x}\right)}{1+B_1\left(-\frac{\mathrm{d}E}{\mathrm{d}x}\right)+B_2\left(-\frac{\mathrm{d}E}{\mathrm{d}x}\right)^2} \qquad (4)$$

(from [9]), where $(-\mathrm{d}E/\mathrm{d}x)$ is given by equation (1) without the Z^2 term. Table 1 shows the adopted numerical values for the used parameters.

6. Time of flight measurement

The single channel time resolution is [2]:

$$\sigma(x) = \sqrt{\frac{\sigma_1^2}{N}+\frac{\sigma_2^2x^2}{N}+\sigma_3^2}\,, \qquad (5)$$

where x is the particle crossing point distance from the photomultiplier (PM), N the number of photoelectrons produced by the light flash in the PM, σ_1 depends upon the PM signal shape and the trigger electronics, σ_2 comes from the dispersion of the photons path length and σ_3 refers to the electronic noise.

The time resolution of a plane is an average over all its channels resolutions, and actually it is determined by its central counters resolution. Assuming no sensible difference between different planes, it is possible to measure their time resolution by looking at the time of flight of ultrarelativistic particles between two given planes, after the correction for their incident angle.

Due to the increasing number N of photoelectrons produced by nuclei with higher and higher atomic number, the time resolution is expected to decrease until it reaches the minimum value σ_3, dictated by the

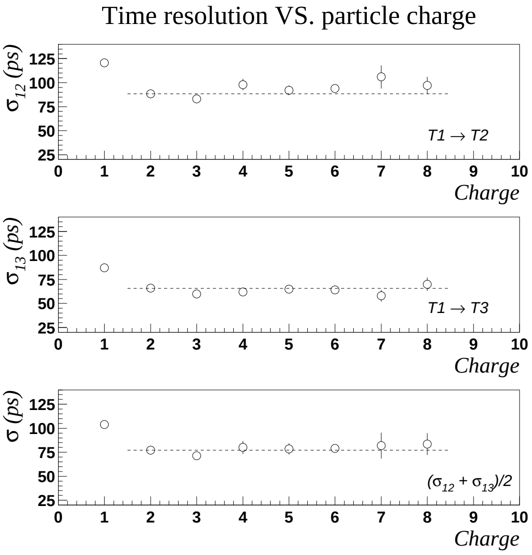

Figure 9. Single plane time resolution from the time of flight between the first and the second (σ_{12}) or the third (σ_{13}) TOF plane, and the mean time resolution.

electronic noise. Figure 9 shows the measured values for the time resolution measured using the first and the second or the third TOF plane: the horizontal lines show that the level of the electronic noise is 88 ps for the first measurement and 66 ps for the second one, leading to a mean value of 77 ps.

6.1. Velocity and position resolution

The position along any counter is computed using the difference between the two time measurements done by the photomultipliers in both ends, and the effective light speed in the scintillator, measured during the TOF calibration (see [2]). The crossing positions, for a given TOF counter, form two box distribution corresponding to its height (1 cm) and width (11 cm), and a gaussian distribution along its longitudinal axis with $\sigma_s \lesssim 2\,\text{cm}$ as shown in figure 10.

With a time of flight resolution of $\sigma_t \lesssim 120\,\text{ps}$, independent from particle direction and rigidity, the TOF system can measure with reliability (say, within 2 standard deviations) velocities with $|\beta| \le \beta_{\max}$, where $\beta_{\max} \approx 0.95$, as can be seen in figure 11.

The variable $\alpha \equiv 1/\beta$ is gaussian distributed, with a constant standard deviation of $\sigma_\alpha = 0.03$ (for protons).

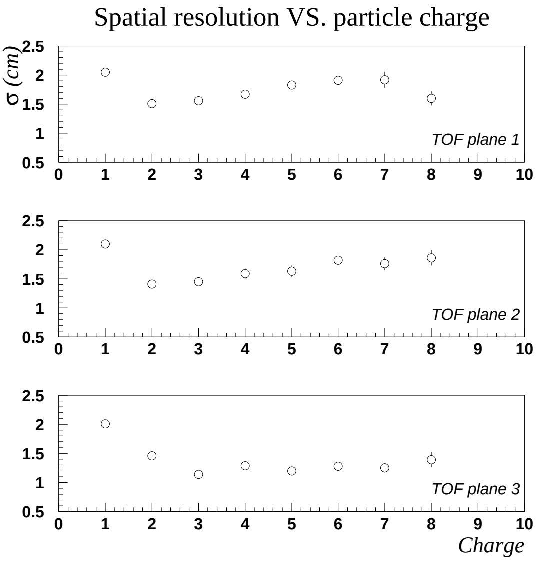

Figure 10. Single plane spatial resolution.

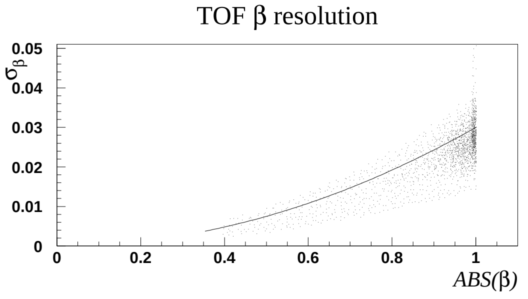

Figure 11. Velocity resolution as function of β.

Hence the uncertainty about β is:

$$\sigma_\beta = \beta^2 \sigma_\alpha = 0.03\beta^2 \tag{6}$$

(solid line in figure 11).

6.2. Rigidity resolution

The TOF system can measure the particle rigidity, with a maximum detectable rigidity of few GV.

One can write the rigidity as function of the particle β and the mass to charge ratio only:

$$R = \frac{pc}{Ze} = \frac{\beta\gamma mc^2}{Ze} = \frac{mc^2}{Ze}\left[\left(\frac{1}{\beta}\right)^2 - 1\right]^{-1/2} . \tag{7}$$

If $m = Am_\text{u}$, where A is the nucleus mass number and m_u is the atomic mass unit ($m_\text{u}c^2 = 931.494\,\text{MeV}$), we

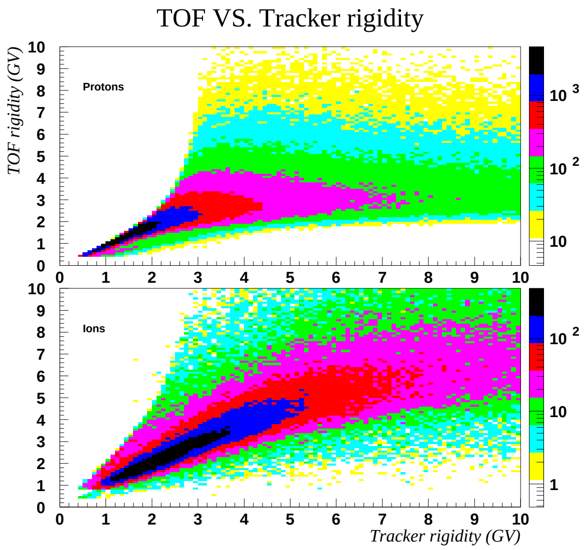

Figure 12. Rigidity measured by the TOF system and the tracker, for protons and ions.

obtain a simple expression for the rigidity (valid only for protons and nuclei):

$$R \approx 0.93 \frac{A}{Z} \left[\left(\frac{1}{\beta} \right)^2 - 1 \right]^{-1/2} \qquad \text{(GV)} , \qquad (8)$$

where $A/Z \approx 1$ for protons and $A/Z \approx 2$ for the light nuclei. The TOF system can separate protons from other cosmic rays ions within 1%, so that the rigidity depends upon β only.

Neglecting the uncertainty on the A/Z ratio, the rigidity resolution is:

$$\sigma_R = m_\mathrm{u} c^2 \frac{A}{Z} \frac{\sigma_\alpha}{8} R^2 \sqrt{R^2 + 4} \, , \qquad (9)$$

where $\alpha \equiv 1/\beta$ is gaussian distributed with $\sigma_\alpha = 0.03$. The maximum detectable rigidity is found imposing $\sigma_R = R$ or putting $\beta = \beta_\mathrm{max}$ in eq. (7), getting $R_\mathrm{max} \approx 2.8\,\mathrm{GV}$ for protons and $R_\mathrm{max} \approx 5.7\,\mathrm{GV}$ for other nuclei. Figure 12 shows the rigidity measured by the TOF system and the tracker.

6.3. Angular resolution

By fitting with a straight line the positions given by the TOF system, it is possible to find out the incident particle direction, written in terms of the colatitude θ and the azimuth ϕ angles.

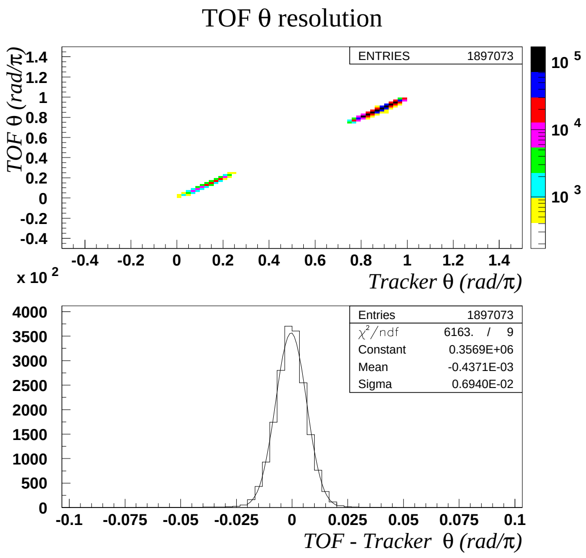

Figure 13. Colatitude measured by the TOF system and the tracker.

The colatitude can be obtained without any problem, as shown in figure 13, with a resolution of $\sigma_\theta = 0.07\,\mathrm{rad}$, over a non-gaussian background at a level of about 1%.

The finite spatial resolution of the TOF system doesn't allow a fine separation of negative and positive y coordinate when y approaches zero, often resulting in a "jump" of π rad in the determination of ϕ using the arctan function, whose validity range is $(-\pi, \pi)$ rad (see figure 14). Fortunately, this is not a problem at all, because the AMS geometric acceptance makes the ϕ distribution simmetric. Then one can consider simply the angle $\phi \bmod \pi$, obtaining a resolution of 0.02 rad, with a non-gaussian background of about 8%.

7. Conclusion

The time of flight system for the AMS detector, in its STS-91 configuration, not only has proven to be a very fast and efficient triggering system, but also to be able to discriminate between protons and heavier nuclei with a 1% background, and to measure the particle velocity with $\sigma_\beta \lesssim 0.03$ and the crossing position with $\sigma_s \lesssim 2\,\mathrm{cm}$, with a total power consumption of about 150 W and a weight of 250 kg.

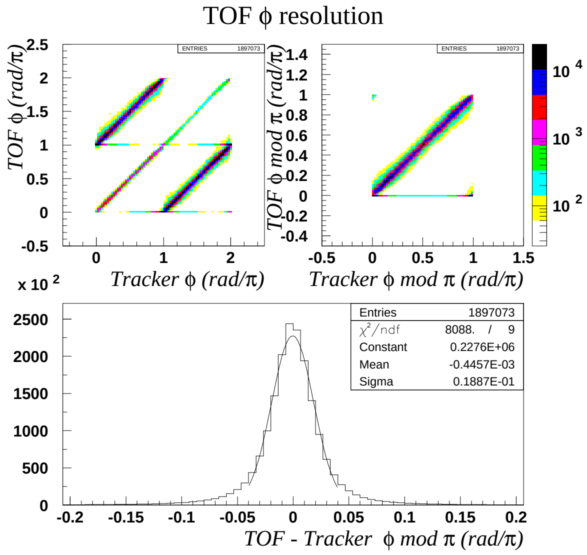

Figure 14. Azimuth measured by the TOF system and the tracker.

REFERENCES

[1]S.P. Ahlen *et al.*, Nuclear Instruments and Methods **A 350** (1994) 351.

[2]D. Alvisi *et al.*, Nuclear Instruments and Methods **A 437** (1999) 212–221.

[3]AMS Bologna Group, “The mechanics for the TOF system of the AMS experiment”, in preparation.

[4]AMS Bologna Group, “Low power, high resolution electronics for the TOF system of the AMS experiment”, in preparation.

[5]L. Brocco, “Search for exotic particles with AMS experiment”, Ph.D. thesis (2001).

[6]C. Caso *et al.*, The European Physical Journal **C3** (1998) 1.

[7]R.M. Sternheimer, Physical Review **88** (1952) 851.

[8]R.M. Sternheimer, M.J. Berger and S.M. Seltzer, Atomic Data and Nuclear Data Tables **30** (1984) 261–271.

[9]W.R. Leo, “Techniques for Nuclear and Particle Physics Experiments”, Springer–Verlag (1987).